

RESEARCH ARTICLE

Assessing Predictive Models for Fairness Based on Movement Patterns

Francesco Lettich^a, Mario A. Nascimento^b, Chiara Pugliese^c and Chiara Renso^a

^aInstitute of Information Science and Technologies, National Research Council, Pisa, Italy;

^bDepartment of Computing Science, University of Alberta, Edmonton, Canada; ^cInstitute of Informatics and Telematics, National Research Council, Pisa, Italy.

ABSTRACT

Assessing the spatial fairness of predictive models involves establishing whether they are statistically penalizing (favoring) individuals associated with certain geographical locations. Literature on this topic makes the fundamental assumption that each individual is assigned to a single geographical location (e.g., place of residence). However, fairness with respect to the set of locations where one has been, i.e., their movement patterns over different regions, also matters when fairness is considered. Consequently, we argue that it is necessary to generalize the notion of spatial fairness to also include *movement patterns*, leading to the novel problem of assessing predictive models for fairness relative to the movements of individuals. To deal with this problem, we propose an approach that first associates the movements of individuals to certain geographic regions, considering multiple spatial partitions with different resolutions and alignments, and then employs a suitable spatial scan statistic to assess whether a predictive model is fair based on movement patterns. In the experimental evaluation, we study the performance of our approach over thousands of synthetic unfair datasets, showing that it is effective at detecting this new type of unfairness and at retrieving the set of objects treated unfairly, while localization performance exhibits a consistent multi-resolution trade-off.

KEYWORDS

Fairness Based on Movement Patterns, Predictive Models, Trajectory, Spatial Scan Statistics, Spatial Fairness

1. Introduction

Fairness in machine learning is a well-established, large, and active research area (Caton and Haas 2024), that addresses the concern that predictive models, whether due to characteristics in the training data or the training process, can be systematically biased towards (or against) certain subsets of a population, due to improper use of an individual's *protected attributes*. A classic example is gender bias in hiring models. *Spatial fairness* is a recently explored variant of fairness (Yan and Howe 2021, Xie *et al.* 2022, Sacharidis *et al.* 2023, Saxena *et al.* 2025) that makes the assumption that every individual is tied to *one fixed geographical location* (e.g., place of residence) and focuses on whether a model penalizes (or favors) individuals in specific geographic areas more than it would be expected by chance. In other words, spatial fairness is based on the premise that one's location should also be considered a protected attribute as it might act as a *proxy* for protected attributes. For example, a model might indirectly (and possibly incorrectly) correlate socioeconomic status, ethnicity, or family structure based on where

one lives or works. Such inferred correlation is the main reason why it is important to *assess* the spatial fairness of a predictive model, as it may indicate the need to *audit* the whole process, from data gathering, cleaning, and processing to decision making. Note that while previous related research, e.g., (Sacharidis *et al.* 2023), has used the term *auditing* we prefer to use the narrower term *assessment*, as the former suggests investigating compliance to a broader standard, which is not our goal.

Existing research on spatial fairness generally takes two complementary directions: one aims to design predictive models that minimize spatial unfairness from the outset (Yan and Howe 2021), while the other focuses on assessing existing predictive models for spatial fairness (Sacharidis *et al.* 2023, Xie *et al.* 2022). In this work, we focus on the latter.

As mentioned before, a key assumption in spatial fairness is that each individual is tied to one single fixed location, but in many real-world scenarios, people move and have habits. This leads to the need to generalize the current notion of spatial fairness to one that encompasses *movement patterns* as well. In other words, movement patterns ought to be considered as a protected attribute, leading to the *problem of assessing predictive models for fairness based on movement patterns*. This applies to predictive tasks where a predictive model considers, as input, among different types of data, the movements of individuals, and the model might treat certain individuals differently because of their movement patterns.

For instance, consider an individual who regularly commutes between home and work and frequently stops in a particular neighborhood to refuel or purchase groceries. Such a neighborhood may be close to places of worship associated with a given religion, or it may offer lower prices because it is located in an economically disadvantaged area. Even if predictive models (correctly) do not consider one’s protected attributes, a model that considers one’s movement patterns may correlate such regular stops with attributes that should be otherwise protected, e.g., religion or income level. That, in turn, can lead to unfair decisions and trigger, e.g., alerts for special surveillance (in the case of predictive policing (Ensign *et al.* 2018)) or denial of a loan (in the case of a financial institution). Recall that the current notion of *spatial fairness* makes the assumption that the individual is associated with a single fixed location. There is no clear notion of the “right location” to use as such, therefore it is very possible that depending on the location chosen, current approaches to detect spatial fairness will fail even though the model’s outcome may be unfair due to the overall movement of said individual. Hence the need to consider *movement patterns*.

There are three dimensions of movement patterns that existing assessment approaches targeting spatial fairness do not capture:

Dimension #1: Multiple locations/regions.

This is due to the very nature of an individual’s movements, i.e., they are bound to be in different regions of the space of interest at different points in time.

Dimension #2: Frequency of visits to different locations.

It does not suffice to consider that an individual was in given regions, but also how often that was the case.

Dimension #3: Duration of visits to each location.

Related to the second dimension, it is also relevant how long one was at a given location.

The first one is key to the distinction between spatial fairness and fairness based on movement patterns. The other two introduce the previously unaddressed temporal aspect to the *spatial fairness* problem, and allow proper consideration of relevant nuances

related to one’s movement patterns. For instance, it may be more meaningful to associate a person with a region they visit regularly for some time, e.g., those containing their home, workplace, supermarket, gym, etc., than those associated with a gas station or a diner they visit rarely and/or briefly.

The remainder of the paper is organized as follows. Section 2 discusses related work, noting that, to the best of our knowledge, none of them can address the problem we propose. Based on the motivation and identification of the research gaps introduced above, Section 3 establishes the necessary background for our proposed approach to be presented. Section 4 presents the main contribution of this paper, namely, an approach that first associates individuals with the geographical regions that are relevant to their movement patterns, and then uses a suitable spatial scan statistic to find out if there are individuals sharing certain movement patterns that are treated unfairly. In the experimental evaluation (Sections 5 and 6), we first explain why thousands of unfair synthetic datasets are needed to evaluate our approach, and how to generate them, noting that our work is the first to propose a generation protocol tailored to unfairness based on movement patterns. We then use these datasets to study the effectiveness of the proposed approach with respect to several parameters. We show that it can effectively detect the presence of unfairness, retrieve the set of objects treated unfairly, and, depending on how the space is partitioned, localize it satisfactorily. Finally, we outline a practical exploratory strategy for real-world assessments and illustrate its application through an example (Section 7).

2. Related work

Fairness in machine learning has been an active research area concerned with the risk that predictive models may produce biased outcomes for certain subsets of a population. The literature distinguishes between *individual fairness* (Dwork and Ilvento 2018b), which requires that similar individuals be treated similarly, and *group fairness* (Dwork and Ilvento 2018a), which requires that groups sharing a common protected attribute receive statistically comparable treatment. Throughout this work, we use the term fairness to refer to group fairness unless otherwise stated. In Appendix A we provide a formal definition of group fairness.

Spatial fairness is a variant of fairness where location is considered as the protected attribute, observing that it can act as a *proxy* for other protected attributes (e.g., race or income). In the following, we focus on works that assess the spatial (group) fairness of existing predictive models. Xie *et al.* (2022) propose a measure that assesses spatial fairness by evaluating how a classifier’s performance varies across multiple geographic subdivisions. To mitigate the Modifiable Areal Unit Problem (MAUP), which is related to the fact that spatial analysis results can change depending on the scale and boundaries of the chosen partitions, the measure repeats this evaluation over many different partitions and summarizes the results as the average variance of the classifier’s performance across them. However, this measure is sensitive to uneven spatial distributions of labeled data and requires access to ground truth labels, limiting its applicability. Furthermore, it does not account for the fact that poor predictive performance in a region can be due to causes unrelated to fairness, e.g., limited local training data, noisy labels, or distribution shift. Finally, predictive performance and fairness can actually be competing objectives, and sacrificing the former might be required (Dwork and Ilvento 2018a, Friedler *et al.* 2019, Shaham *et al.* 2022).

Sacharidis *et al.* (2023) propose a statistically grounded approach to assess binary

classifiers for spatial fairness. Their approach uses the Bernoulli-based spatial scan statistic from Kulldorff (1997), previously used to detect hotspots of diseases, to instead find out the regions in which the proportion of positive labels deviates significantly from the proportion outside. To mitigate the MAUP, their approach also supports using the statistic considering multiple different tessellations. The authors did not quantitatively evaluate the detection and localization performance of their approach; while this can be justified by the fact that they apply the spatial scan statistic of Kulldorff (1997) as is, it remains unclear to what extent their approach is MAUP-resistant, and they did not provide principled guidelines on how to choose the tessellation resolutions.

A subsequent work (Saxena *et al.* 2025) builds on (Sacharidis *et al.* 2023) with a key observation: statistical unfairness can actually be justified. It then assumes that information concerning the protected and non-protected attributes of individuals are known and, for any cell in any tessellation over the area of interest, their approach derives two vectors: one related to the protected attribute and the other to the non-protected ones of the cell’s individuals. They then identify pairs of cells that are similar in the non-protected attributes but dissimilar in the protected one, and identify the pairs whose outcome distributions differ substantially using a modified version of the Bernoulli-based spatial scan statistics, which compares pairs of regions rather than a region against the rest of the space. (Saxena *et al.* 2025)’s approach relies on task-dependent similarity metrics that may require deep and ad-hoc domain knowledge to define. Moreover, while the approach is claimed to be MAUP-resistant, it still remains vulnerable to adversarial repartitioning that dilutes unfair outcomes by merging affected areas with neighboring fair ones; furthermore, no principled guideline on how to choose the tessellation resolutions was provided. Finally, the authors did not measure the detection and localization performance of their approach, which is standard practice when proposing a new spatial scan statistic (Read *et al.* 2011, Kulldorff *et al.* 2009, Jung *et al.* 2010).

To the best of our knowledge, our work differs from previous literature on spatial fairness as it considers the problem of assessing predictive models for fairness based on the movement patterns of individuals, which requires to go beyond the basic assumption that each individual is associated with a single fixed location.

3. Preliminaries and problem definition

In this section, we review some fundamental concepts that will be used throughout the rest of the paper, and introduce the problem addressed in this work. We denote the set of moving objects by MO and the set of their trajectories by \mathcal{T} . First, we describe the structure that a dataset should have in order to allow assessing a predictive model for fairness based on movement patterns.

Definition 3.1 (Auditable Dataset). Each element in an *auditable dataset* D is a triplet $(mo, T_{mo}, pred_{mo})$, where $mo \in MO$ is a moving object, $T_{mo} \in \mathcal{T}$ is the trajectory describing mo ’s movements, and $pred_{mo}$ is a value predicted by the model for mo .

Before considering the notion of spatial fairness, we first introduce the notion of geographic zoning, which is necessary for identifying *regions* where unfairness by a predictive model might occur.

Definition 3.2 (Geographic zoning). Consider a geographic area of interest that contains all trajectories in \mathcal{T} . Suppose that within such an area we define a set of polygonal cells GZ that partitions the area into disjoint regions, e.g., a uniform grid. We refer to

any such set GZ as a *geographic zoning* of the area of interest.

From here on, we call the regions where unfairness occurs as *hotspots of unfairness*. We now introduce the notion of *spatial fairness* (Sacharidis *et al.* 2023). From a technical standpoint, it can be viewed as an instance of group fairness targeting statistical parity (Dwork and Ilvento 2018a, Friedler *et al.* 2019) where we consider the location an object is associated with as the protected attribute.

Assessing for spatial fairness also requires dealing with the Modifiable Areal Unit Problem (MAUP) (Wong 2004, Xie *et al.* 2022, Sacharidis *et al.* 2023), i.e., the spatial analysis results can change with the scale and zoning/boundaries of the chosen spatial partitions¹. Consequently, we use several different geographic zonings $\mathcal{GZ} = \{GZ_1, \dots, GZ_q\}$ to deal with the MAUP; let us focus on a single geographic zoning GZ . Establishing which subset of cells in GZ should be assigned to each moving object, based on their spatiotemporal behavior and/or domain-oriented certain spatial and temporal thresholds, is not a trivial task, mainly due to the three dimensions posed in Section 1.

Furthermore, in the context of assessing fairness based on movement patterns, the MAUP becomes even more complex, as it needs to be considered under the light of a moving entity, unlike in the case of conventional spatial fairness, which assumes that each entity is associated with a single fixed location. Indeed, when fairness is assessed through movement patterns, a moving object may be associated with multiple geographically distinct regions, and a predictive model may treat objects that share the same combination of such regions differently. Consequently, under our notion of unfairness, a hotspot may consist of multiple separate regions rather than a single contiguous one.

Definition 3.3 (Moving object-to-cell association). Given a set of moving objects MO , their trajectories \mathcal{T} , and a geographic zoning $GZ \in \mathcal{GZ}$, we define an *association function* $asc : MO \rightarrow 2^{|GZ|}$ that maps each moving object $mo \in MO$ to a subset of cells in GZ according to the characteristics of its trajectory $T_{mo} \in \mathcal{T}$.

How to instantiate the function asc will be discussed while presenting our approach in Section 4. We are now ready to state the problem addressed in this work.

Problem Statement. Given an auditable dataset D , a set of geographic zonings \mathcal{GZ} over an area of interest, and a moving object-to-cell association function asc , our goal is to identify whether there are subsets of cells in any $GZ \in \mathcal{GZ}$ whose associated moving objects are *statistically treated differently*² by the model because of their movement patterns, relative to the other moving objects.

4. The proposed approach

Next, we present our proposed approach to assess predictive models for fairness based on movement patterns. The approach is structured in five distinct steps. First, it *segments trajectories into stop and move segments* (Section 4.1). Stop segments correspond to parts of a trajectory where an object remained around a certain location for some time, while move segments capture transitions between stops. Subsequently, our approach *superimposes* several *geographic zonings*, i.e., spatial partitions, using different

¹Appendix B provides an illustrative example.

²This means that for the moving objects associated with any subset of cells of a given geographic zoning, the model's predicted values deviate significantly from the others, as established by a suitable hypothesis test.

resolutions and alignments, over the area containing the segments (Section 4.2). This is done to mitigate the Modifiable Areal Unit Problem (MAUP) (Wong 2004, Xie *et al.* 2022, Sacharidis *et al.* 2023), as considering multiple partitions reduces this risk.

The approach then repeats the following two steps for each partition. It first performs *object-to-cells mapping* (Section 4.3), i.e., it maps each moving object to the subsets of cells it is regularly associated with. Subsequently, it uses this mapping to *compute the subsets of cells that must be assessed* for fairness (Section 4.4). After this, the approach applies a suitable *spatial scan statistic on such subsets*, to assess whether and where the model violates fairness based on movement patterns; and *returns the evidence* (if any) allowing the user to further investigate the potential bias (Section 4.5).

Finally, we conclude this section by showing how our assessment approach can reduce to the one from Sacharidis *et al.* (2023) under the spatial fairness assessment scenario (Section 4.6).

4.1. *Trajectory segmentation*

Our approach begins by instantiating the *object-to-cells association* function asc introduced in Definition 3.3, thus starting to address the three dimensions outlined in Section 1. Recall that this function must map each moving object to a subset of geographic areas that meaningfully characterize their movement behaviors.

To discover such areas, our approach first performs an operation known as *trajectory segmentation*, using the well-known *stop-and-move* criterion (Spaccapietra *et al.* 2008). A stop segment represents a specific part of a trajectory during which the associated moving object *stayed* in a *specific area* for *some time*. The move segments are simply parts of a trajectory that are not stop segments. In this work, we focus specifically on the stop segments and use the algorithm from (Hariharan and Toyama 2004) to find them. We adopt a person-based perspective in which we aim to identify the geographic locations where an individual frequently stays, that is, the stop *locations that consistently structure most of their routines*. Typical examples include home, work, school, gym, preferred supermarkets or restaurants, and more.

Formally, we represent each stop segment as a quadruple $st = (mo, l, t_{start}, t_{end})$, where mo is the identifier of the moving object, or individual, l is the location of the centroid of the stop segment and t_{start}, t_{end} its starting and ending instants of the stop, respectively. We finally denote the set of all detected stop segments as $STOP = \{st_1, \dots, st_m\}$, where m is the total number of stops detected across all moving objects' trajectories in the auditable dataset D .

4.2. *Superimposing multiple geographic zonings*

Following the terminology introduced in Definition 3.2 and considering the modifiable areal unit problem (MAUP), this step superimposes q different geographic zonings $\mathcal{GZ} = \{GZ_1, \dots, GZ_q\}$ over the geographic area containing the locations associated with the stop segments. A natural question is then: how to select an appropriate number of zonings q ? In practice, this requires deciding how many different resolutions and alignments one wants to use to mitigate the MAUP.

Part of this choice concerns the *coarsest* grid resolution, and is informed by some spatial scan statistics literature (Kulldorff 2001) which suggests constraining the size of the cells to contain at maximum 50% of the total population. This excludes zonings that are, e.g., too coarse. The remaining choices concern the *finest* and *intermediate*

grid resolutions. These depend on the size and structure of the geographic area under study, the spatial scales at which meaningful movement patterns may arise, and the available computational budget. In general, the finest resolution should reflect the smallest relevant geographic unit in the considered area, such as a city block in an urban setting. The intermediate resolutions should cover the range between the finest and coarsest resolutions, so that hotspots can be detected at multiple spatial scales. As for the alignments, one should use a fixed number of shifts for each chosen resolution to better capture hotspot boundaries.

4.3. Object-to-cells mapping

This step takes as input the stop segments computed in the previous trajectory segmentation step and a single geographic partition $GZ \in \mathcal{GZ}$, and addresses the problem of associating each moving object with the set of geographical regions (cells) in GZ that characterize their movements. This is again connected to dealing with the three dimensions from Section 1, as people’s movements typically intersect multiple regions. Depending on how frequently and for how long people visit such regions, some of these regions are more relevant than others.

Our approach performs this mapping by analyzing where and when the stop segments occur within the cells of the geographic zoning. Let $STOP_{mo} \subseteq STOP$ be the set of stop segments for the moving object mo . We first perform a spatial join between the centroids of the stop segments and the cells in GZ based on the *intersection* predicate:

$STOP_{mo}^{ann} = STOP_{mo} \underset{\text{intersect}}{\overset{\text{spatial}}{\bowtie}} GZ$. This generates a set of annotated stops, $STOP_{mo}^{ann}$,

where each stop segment becomes a quintuple $(mo, l, cell, t_{start}, t_{end})$, and allows us to identify the subset of cells in GZ that contain at least one of mo ’s stop segments. We denote this subset as GZ_{mo} .

Notice that not all cells touched by a moving object’s stop segments are equally meaningful. For example, one cell may contain a place of worship, with repeated long stays, while another may include only a single occasional stay, e.g., the person visited a new restaurant to try it out; clearly, these regions carry different relevance. To identify the most relevant regions, we apply the following criterion: for every cell in GZ_{mo} , we count the *number of distinct days* temporally intersecting one or more of the stop segments of mo in that cell. Intuitively, the more distinct days in which a cell occurs in a person’s life, the more that cell is relevant to the person’s movement patterns. Note that while in this paper we adopt “distinct days” as a unit of interest, other units can be used without prejudice to the proposed approach.

This criterion ultimately induces a ranking over the cells in GZ_{mo} , thus addressing the aforementioned three dimensions characterizing our problem. We then select the top- i cells from GZ_{mo} and define them as the *cellset* of mo . We denote this set by GZ_{mo}^i and use it in the subsequent steps of the assessment process. The parameter i acts as a cut-off: it determines how many cells are deemed relevant for each moving object. In practice, i should reflect the typical number of meaningful places in people’s routines, with some margin for variability (e.g., $i = 8$). This last operation terminates the instantiation of the *object-to-cells association* function asc introduced in Definition 3.3. Finally, recall that the sequence of operations just described is repeated for every zoning $GZ \in \mathcal{GZ}$.

4.4. Determining the subsets of cells to assess

For each partition $GZ \in \mathcal{GZ}$, this step takes as input the cellsets computed for the moving objects in the previous step, and computes the subsets of cells that must undergo hypothesis testing. More precisely, we aim to find subsets of cells that occur at least once among the moving objects' cellsets. The main challenge in solving this problem lies in the size of the search space. Each moving object's cellset is made up of up to i cells, and cellsets can intersect in many different ways; thus, if GZ is the partition currently considered, then $|GZ|$ is the number of cells in this particular partition, and the search space has exponential size $O(2^{|GZ|})$. Consequently, efficiently exploring this space, both in terms of memory and computation, is crucial.

To address this problem, we use techniques from the well-known *frequent itemset mining* (FIM) literature (Agrawal *et al.* 1996, Zaki 2002), effectively casting the problem faced in this step as a variant of FIM. Accordingly, we first provide a brief introduction to the FIM problem, adopting the terminology from one of the seminal works in the literature (Zaki 2002). In FIM, one is given a typically large database of transactions where each transaction contains a set of items. The goal is to discover the so called *frequent itemsets*, i.e., subsets of items whose *support*, i.e., number of transactions they occur in, is above a given threshold. For example, in market basket analysis, each transaction represents the products bought by a customer, and finding the frequent itemsets across many transactions means finding the sets of products that customers often buy together. Going back to our problem, we can cast it as an FIM variant as follows:

- Each moving object's cellset, GZ_{mo}^i , can be seen as a transaction uniquely identified by the object's identifier;
- Each cell can be seen as an item that appears in at least one cellset (transaction);
- The *support* of a cell is equal to the number of cellsets in which it occurs;
- From the FIM literature (e.g., lemma 5 from (Zaki 2002)), itemsets (subset of cells) can be *joined* into larger itemsets by taking their set-union; and the IDs of the transactions associated with a joined itemset are obtained by set-intersecting the sets of IDs associated with the two itemsets being joined;
- Therefore, the *support* of a *subset of cells* is equal to the number of moving objects whose cellsets contain the subset.

Thus, the problem is to identify all subsets of cells in GZ with support at least one, i.e., all subsets associated with at least one object, and denote the resulting set by $CANDIDATES_{GZ}$. We intentionally retain all such subsets so as not to exclude sparsely represented areas or movement patterns, while subsets with zero support are untestable and thus discarded. The algorithm implementing this step has the same key characteristics as the Eclat candidate generation algorithm from (Zaki 2002). Appendix C provides more details on the algorithm and this step's complexity.

4.5. Hypothesis testing

This step returns to considering all the zonings in \mathcal{GZ} , and aims to determine whether there is statistically significant evidence of unfairness based on movement patterns by the predictive model for any subset of cells in $CANDIDATES_{\mathcal{GZ}} = \{CANDIDATES_{GZ_1} \cup \dots \cup CANDIDATES_{GZ_q}\}$, according to the predicted values available in the auditable dataset D . Let us denote the set of predicted values in D as $PRED$. We resort to a well-established family of well-known

spatial scan statistics (Kulldorff 1997, Kulldorff *et al.* 2009, Jung *et al.* 2010). While the specific spatial scan statistic required depends on the predictive model being assessed, the high-level testing methodology is as follows:

Stage 1: State the null hypothesis H_0 and alternative H_1 . The null hypothesis H_0 posits that the model being assessed is fair, i.e., all moving objects share the same global distribution for the predicted values. The alternative H_1 posits that there is at least a set of moving objects associated with a subset of cells $c \in CANDIDATES_{GZ}$ for which the distribution of their predicted values differs from that of the other objects.

Stage 2: Choose the spatial scan statistic appropriate for the model being assessed. A test statistic T is a function that maps the observed data (predicted values) to a scalar, and is used to decide whether to reject the null hypothesis H_0 or not. The family of spatial scan statistics from Kulldorff *et al.* that we consider in this work employs the *maximum likelihood ratio* (MLR) as T . Each of these statistics instantiates the MLR according to the parametric probability model appropriate for the predictive model being assessed, e.g., a Bernoulli-based statistic for binary classifiers (Kulldorff 1997), a multinomial-based statistic for multi-class classifiers (Kulldorff *et al.* 2009), and a Normal-based statistic for regressors (Jung *et al.* 2010).

In general, the MLR requires maximizing two likelihood functions L_0 and L_1 that formally represent H_0 and H_1 , respectively, and are defined using the chosen parametric probability model. They express how plausible the observed data is under each hypothesis when using specific parameter(s) for the probability model. Maximizing L_0 and L_1 yields L_0^{max} and L_1^{max} , which lead to the MLR:

$$T = \frac{L_1^{max}}{L_0^{max}}$$

The larger T , the more the predicted values favor H_1 over H_0 , i.e., the moving objects associated with some $c \in CANDIDATES_{GZ}$ are treated differently beyond mere chance. Note that a single value of T does not determine whether to reject H_0 . We also need the distribution of T under the assumption that H_0 is true. In spatial scan statistics, this is approximated through Monte Carlo simulations, obtaining T 's *null distribution* (see Stage 6). We then compute T on the actual predicted values $PRED$, and see where it falls in the null distribution to decide whether to reject H_0 (Stages 7 and 8).

Stage 3: Formalize H_0 . H_0 is formalized with the likelihood function $L_0(\theta; VALUES)$, which uses the analytical form of the chosen parametric probability model to measure how plausible the data in $VALUES$ are under the assumption that there is a single global distribution over the predicted values. The goal is to find the specific θ that maximizes L_0 :

$$L_0^{max}(VALUES) = \max_{\theta} L_0(\theta; VALUES).$$

Stage 4: Formalize H_1 . We still use the same probability model, but use it twice when defining L_1 : one for the moving objects associated with some $c \in CANDIDATES_{GZ}$, with input parameters θ_{in} , and another for the other objects, with input parameters θ_{out} . Hence, we get $L_1(\theta_{in}, \theta_{out}, c, VALUES)$. Analogously to L_0 , the goal is to maximize L_1 , but with an additional step: we must first maximize L_1 separately for each $c \in$

$CANDIDATES_{\mathcal{GZ}}$

$$L_1^{max}(c, VALUES) = \max_{\theta_{in}^c, \theta_{out}^c} L_1(\theta_{in}^c, \theta_{out}^c; c, VALUES),$$

and finally, find out the c that yields the largest value

$$L_1^{max}(CANDIDATES_{\mathcal{GZ}}, VALUES) = \max_{c \in CANDIDATES_{\mathcal{GZ}}} L_1^{max}(c, VALUES).$$

In essence, H_1 is a composite alternative stating that there exists at least one subset $c \in CANDIDATES_{\mathcal{GZ}}$ for which $\theta_{in} \neq \theta_{out}$.

Stage 5: Choose a statistical significance level α . It represents the probability that we accept rejecting H_0 when it is actually true.

Stage 6: Compute an approximated distribution of the test statistic under H_0 via Monte Carlo Simulations. Following standard practice in spatial scan statistics, we derive an approximation of T 's distribution from the predicted values in $PRED$ under the assumption that H_0 is true. More specifically, we conduct n Monte Carlo simulations: in each simulation $b \in \{1, \dots, n\}$, we generate a synthetic dataset of predicted values $PRED_b$ by randomly shuffling the values in $PRED$. The approximated null distribution of T is then obtained by computing for each simulation b the MLR:

$$T_b = \frac{L_1^{max}(CANDIDATES_{\mathcal{GZ}}, PRED_b)}{L_0^{max}(PRED)}.$$

Concerning $L_0^{max}(PRED)$, recall that H_0 postulates that there is just a single global probability distribution over all the moving objects' predicted values. Thus, shuffling the values in $PRED$ does not change such a distribution, hence $L_0^{max}(PRED)$ can be computed once and shared across all the simulations. However, $L_1^{max}(CANDIDATES_{\mathcal{GZ}}, PRED_b)$ must be computed for each simulation, as it depends on the shuffled values and the partition $GZ \in \mathcal{GZ}$ being considered. Ultimately, $T^{H_0} = \{T_1, \dots, T_n\}$ provides the approximated null distribution.

Stage 7: Compute the test statistic over the original predicted values in $PRED$. From $PRED$ and the set of subsets of cells to be tested in $CANDIDATES_{\mathcal{GZ}}$, compute the scalar:

$$T_{obs} = \frac{L_1^{max}(CANDIDATES_{\mathcal{GZ}}, PRED)}{L_0^{max}(PRED)}.$$

Stage 8: Determine whether to reject H_0 . With T^{H_0} and T_{obs} , we can estimate the probability under H_0 of observing a MLR *at least as extreme as* T_{obs} , i.e., $\hat{p} = \Pr(T \geq T_{obs} | H_0)$. This is also known as the right-tailed p -value of T_{obs} . Subsequently, we compare \hat{p} to the significance level α and reject H_0 if $\hat{p} \leq \alpha$. Intuitively, the larger (more extreme) T_{obs} is compared to the top-values in the sorted T^{H_0} , the stronger the evidence of unfairness. Concretely, we first determine the p -value of T_{obs} as its rank in T^{H_0} :

$$\hat{p} = \frac{1 + \sum_{T_b \in T^{H_0}} \mathbb{1}(T_b \geq T_{obs})}{n + 1},$$

where $\mathbb{1}(\cdot)$ represents the indicator function and n the number of simulations. Then, if

$\hat{p} \leq \alpha$ we *reject* H_0 in favor of H_1 .

Stage 9: preparing the evidence for further analysis. If H_0 is rejected, then there is at least a subset of cells for which there is evidence of unfairness, and others might exist. Hence, for each $c \in \text{CANDIDATES}_{\mathcal{GZ}}$ we consider $T_c = \frac{L_1^{\max}(c, \text{PRED})}{L_0^{\max}(\text{PRED})}$ – observe that $L_1^{\max}(c, \text{PRED})$ has already been computed for $L_1^{\max}(\text{CANDIDATES}_{\mathcal{GZ}}, \text{PRED})$ in Stage 7 – and find its rank in T^{H_0} to verify if it exceeds α : all the subsets that satisfy this condition are stored in $\text{UNFAIR}_{\mathcal{GZ}}$.

Appendix D provides additional considerations regarding the complexity of this step, while Appendix E provides some considerations about the overall complexity of our approach.

4.6. *Reduction to the standard spatial fairness assessment case*

It is worth noting that our approach is also capable of evaluating the spatial fairness of a predictive model under the scenario considered in (Sacharidis *et al.* 2023); thus, being more generic. Recall that in that more constrained scenario, each object is associated with a single point. Therefore, the *trajectory segmentation* step is unnecessary and can be skipped. Our approach still executes the step that *superimposes multiple geographic zonings* with different resolutions and alignments, over the area containing the points. Next, for each geographic zoning, the *object-to-cells* mapping step reduces to a spatial join (using the intersection predicate) between the points and the cells of the zoning, while the step that *determines* the subsets of cells that *must undergo hypothesis testing* also simplifies, since it only needs to identify the cells that contain at least one point. Finally, the hypothesis testing recipe remains unchanged.

5. Experimental setting

In this work, we instantiate the experimental evaluation for the case of assessing a binary classifier for fairness based on movement patterns. Section 5.1 describes why we need to generate synthetic unfair auditable datasets, and how we generate synthetic movement data through a simulator. Section 5.2 introduces the protocol we use to generate thousands of unfair auditable datasets from said movement data. Section 5.3 presents the measures used to evaluate our assessment approach. Finally, Section 5.4 details the parameters used to configure the approach for the experimental evaluation.

Although our experimental evaluation focuses on assessing a binary classifier, we highlight that our approach is not limited to this case. In order to consider other types of predictive models, it would require (1) using a spatial scan statistic in the hypothesis testing in Section 4.5 that is appropriate for the model being assessed; (2) adjusting the protocol so that unfairness is injected considering a type of distribution that is appropriate for the values outputted by the model; and (3) repeating the empirical evaluation on the newly generated unfair datasets. In essence, our approach remains the same, what changes are the spatial scan statistics and the protocol to generate unfair datasets.

The source code behind this work is available at: <https://github.com/Fr4nz83/AuditMovementFairness>. The datasets used in this work and the intermediate data generated by the proposed approach are available at: <https://figshare.com/s/93b04d0a6128d3e7ca32>.

5.1. Generation of synthetic movement data

To the best of our knowledge, there are no real auditable datasets that meet the needs of our evaluation. As established in the spatial scan statistics literature (Read *et al.* 2011, Kulldorff *et al.* 2009, Jung *et al.* 2010), estimating the detection and localization performance of an approach³ that uses a spatial scan statistic requires to use measures that evaluate an approach over large collections of datasets with known ground truth – we detail these measures in Section 5.3. We therefore need to generate multitudes of synthetic auditable datasets. We do this by first generating synthetic movement data, which we then use as the basis to generate unfair auditable datasets. The idea is to keep the movement data fixed, while unfairness is injected via the objects’ labels (i.e., the predicted values).

We generate the movement data using the *Patterns of Life* simulator from Züfle *et al.* (2023). We simulate 100,000 individuals living in the city of Atlanta, Georgia, USA. Their movements follow well-defined behavioral patterns that reflect basic human needs, such as commuting between home, work, supermarket, restaurant, and more. Figure 1 shows a heatmap based on a random sample of 1 million trajectory points drawn from the original 720,199,539, in which we notice their uneven spatial distribution. The sampling rate of the trajectories is 2 minutes. The temporal interval spanned by the trajectories is 10 days. The bounding box enclosing the trajectory samples has a width of 4.69 kilometers and a height of 4.83 kilometers. From here on, we refer to the simulated individuals as objects.

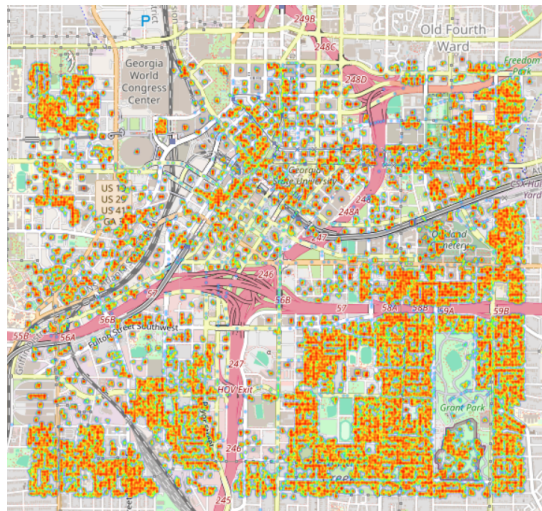


Figure 1. Heatmap of a million trajectory samples where the red areas denote the locations where the simulated individuals tend to stay.

The simulator generates a very large amount of data, hence we apply the trajectory compression algorithm outlined in (Zheng 2015) and implemented in the scikit mobility library from Pappalardo *et al.* (2022). Briefly, for each object, samples are first ordered by timestamp. Starting from the first uncompressed sample, the algorithm uses it as an anchor point and collects the maximal consecutive sequence of subsequent samples whose distance from the anchor is at most a given *radius*. This sequence is replaced by a single sample whose spatial coordinates are the component-wise median of the coordinates in the sequence and whose timestamp is the timestamp of the anchor sample.

³These metrics are detailed in Section 5.3

The procedure then continues from the first sample outside the radius and is repeated until the trajectory has been fully processed. In our experiments, we set the above radius to one meter in order to remove very short movements, bringing the final number of trajectory points to 19,815,853.

5.2. *Generating unfair auditable datasets: A protocol for injecting unfairness based on movement patterns*

Next, we generate several groups of synthetic unfair auditable datasets from the movement data. The underlying idea is to first associate a fraction of objects to hotspot(s) of unfairness, and then manipulate their labels such that they are treated differently. We argue that unfairness can be injected considering several parameters, and in our work we consider the following ones:

- (1) the *shape* of the regions composing the hotspots;
- (2) the *number of objects associated* with a hotspot;
- (3) the *number of hotspots* in a dataset;
- (4) the unfairness *magnitude*;
- (5) the *number of separate regions* composing a hotspot;
- (6) how objects are *associated* with the hotspots.

Parameters 1 through 4 are inspired by protocols defined in spatial scan statistics literature (Kulldorff 1997, Kulldorff *et al.* 2009, Jung *et al.* 2010), while the last two are due to the necessity of adding movement pattern as a possible cause for unfairness. That is, objects can be associated with multiple locations, rather than a single one as previously assumed, and a predictive model can treat objects associated with a certain set of distinct geographical regions differently. Next, we present the injection protocol we used in this work.

The first parameter is the shape of the regions composing the hotspots. Shapes should be sufficiently varied and differ from those of the cells of the zonings, to not artificially favor an assessment approach. For this reason, we consider the geometries of a subset of the 2025 US Census block groups for the state of Georgia (U.S. Census Bureau, Department of Commerce 2025), more precisely the 51 block groups that cover our simulation area (Figure 2, left plot).

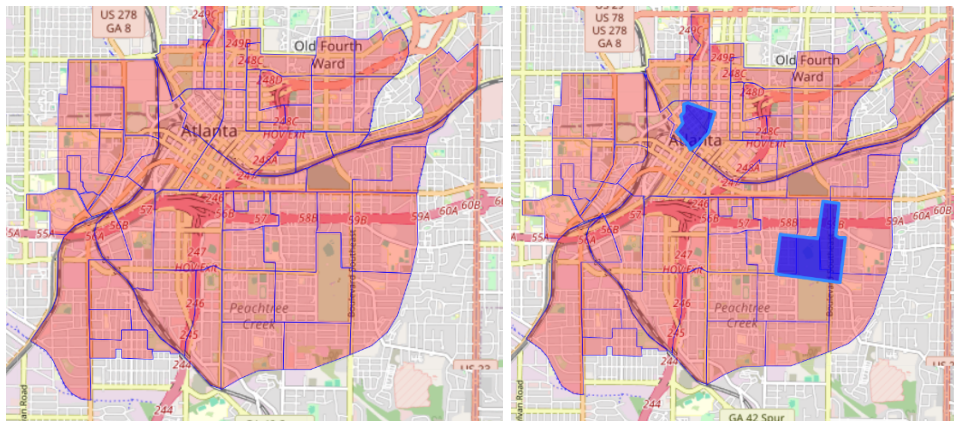


Figure 2. *Left plot:* the subset of 51 US Census block groups intersecting the movement data, shown as red-filled with blue edges. *Right plot:* hotspot made of two separate regions (blue filled polygons) constructed from the original block groups.

More precisely, to construct a hotspot of n distinct regions (second parameter), n distinct block groups are first randomly sampled from the above-mentioned 51, and then undergo the following geometric transformations. Each block group is rotated by a random angle about the centroid of its bounding box, then translated horizontally and vertically by a random offset, subject to the constraint that the transformed polygon still intersects the original’s bounding box. The rotation and translation operations decorrelate the hotspot geometry from the original block group geometry, while the intersection check ensures that the transformed shapes remain geographically localized.

The final transformation we need to apply to the original block groups controls another key parameter, namely the *number of objects associated* with the hotspot. This is an important parameter since even when the magnitude of unfairness is kept fixed, a hotspot involving more objects provides a stronger statistical signal, potentially making the unfairness easier to detect but also increasingly harder to delineate its boundaries.

To achieve this, we consider the areas of the n rotated and translated polygons, and apply the same buffer operation to all of them, shrinking or enlarging their areas until the number of associated objects matches a given target value. Figure 2, right plot, provides an example of a hotspot made of two regions derived from the original block groups. Note that when an exact match is not possible for geometric reasons, we keep the hotspot if the number of objects is sufficiently close to the target. In our evaluation, we allow a maximum absolute difference of 10 objects w.r.t. the target in order to control the variance of this parameter across the generated datasets; otherwise, we discard the hotspot.

Another parameter requires specifying *how objects* become *associated* with a *hotspot*. In our work, we use the centroids of the objects’ stop segments computed from their trajectories. More precisely, an object becomes associated with the region of a hotspot if it has at least a given number of stop centroids within that region. An object is therefore associated with the hotspot if it has that number of stop centroids within each hotspot’s region. The smallest possible value for this parameter is 1, which requires the object to have stopped at least once in every hotspot region. Larger values impose a stronger association since they require repeated stops in each region. This can make detection and localization easier, but, at the same time, the boundaries of the hotspots become increasingly more complex, which can negatively impact precise spatial localization.

Another parameter is the *number of hotspots* into which unfairness is injected. To control this parameter, we simply repeat the generation of a single hotspot the desired number of times.

Finally, the last parameter is the *magnitude* of the injected unfairness, which is controlled by increasing the difference between the distribution of the outcomes of the objects associated with the hotspots and the distribution of the outcomes of the other objects. For binary outcomes, this is equivalent to increasing the difference between their positive-label rates, since a Bernoulli distribution is fully determined by its success probability. For example, suppose that the positive label corresponds to a beneficial decision, such as a loan approval. If the classifier assigns this positive label to 60% of the general population but only to 40% of the individuals associated with a specific movement pattern (hotspot), then that group receives the beneficial outcome 20% less often, which is precisely the unfairness magnitude. In a group-fairness statistical-parity sense, this is the kind of systematic disparity we want to inject and then detect. If the positive label represented an adverse outcome, the interpretation would be reversed, but the magnitude would still be the difference between the two rates.

We now describe how we generate the unfair auditable datasets used in the experiments. Before going ahead, we clarify that we do not treat the shape parameter as an

explicit experimental parameter; instead, each hotspot is generated from block groups that are selected and transformed randomly, as explained before, so variability in this parameter is present within every generated set of datasets. We therefore consider explicitly the other five parameters reported in Table 1, which also list their corresponding ranges and default values. We define a *configuration* of unfair auditable datasets as a set of 1,000 datasets independently generated under the same combination of values for these five parameters. Even within a configuration, datasets still differ because the random choices involved in hotspot construction and label generation vary from one dataset to another.

Overall, we consider 21 configurations, obtained by varying one parameter over its range while keeping the other parameters fixed at their default values. We note that we pick *one* stop per region and *one* hotspot per dataset as defaults for those parameters in order to consider the minimal nontrivial configuration for unfairness based on movement patterns. Using larger values and the resulting increased unfairness complexity are considered when studying those two parameters specifically.

Table 1. Parameters considered when generating unfair auditable datasets.

	Range of values	Default value
Regions per hotspot	{1, 2, 3}	2
Stops per region	{1, 2, 3, 4, 5}	1
Objects per hotspot	[200, ..., 600], step 100	400
Hotspots	{1,2,3}	1
Unfairness magnitude	[0.2, ..., 0.6], step 0.1	0.4

5.3. Evaluation metrics

The assessment approach proposed in this work depends on a family of spatial scan statistics mentioned in Section 4.5. When proposing a new spatial scan statistic, or an approach that uses existing ones (as in our case), one has to evaluate its detection and localization performance.

Detection performance is measured by applying an assessment approach to a group of datasets for which unfairness based on movement patterns is present, and then computing the *fraction* of datasets in which the approach successfully *detects* it. This is also known as estimating the *statistical power* of the approach. This requires to have a *large amount* of datasets, and justifies the need to create several distinct groups of synthetic auditable datasets, where unfairness is *injected* considering several parameters to evaluate the detection performance of an assessment approach under different conditions.

Estimating the statistical power, however, is not enough because it does not quantify how well an approach retrieves the set of objects treated unfairly or how well it *spatially localizes* unfairness. This issue is closely related to the fact that the true shapes of the hotspots of unfairness are typically unknown, as already mentioned when discussing the MAUP in Section 3. Moreover, the fact that a hotspot can be composed of multiple regions further complicates the problem. We therefore borrow two metrics from spatial scan statistics literature, which are used as proxies to evaluate localization performance: *sensitivity* and *Positive Predictive Value (PPV)* (Read *et al.* 2011, Kulldorff *et al.* 2009, Jung *et al.* 2010).

Formally, consider a synthetic auditable dataset in which unfairness is present, and we also know the sets of moving objects treated differently; consequently, let U denote

the set of moving objects truly treated differently, and let \hat{U} denote the set of objects an assessment approach considers treated differently. Note that both U and \hat{U} may contain moving objects from *different* hotspots – in this case, we assume that U and \hat{U} simply represent the set union of the objects associated with the hotspots and the candidates deemed as extreme from the hypothesis test in Section 4.5, respectively. Then, sensitivity measures the fraction of objects truly affected that were correctly detected by an assessment approach, while PPV measures the fraction of objects detected by an assessment approach that truly belong to U :

$$\text{Sensitivity} = \frac{|U \cap \hat{U}|}{|\hat{U}|} \quad \text{PPV} = \frac{|U \cap \hat{U}|}{|U|}$$

These can be viewed as reinterpretations of the classic recall and precision measures, respectively, because they are applied to the objects associated with the hotspots rather than to the hotspots themselves.

In our experimental evaluation, we compute both measures as averages across a given configuration of unfair auditable datasets, but *limited* to the datasets in the configuration in which the approach *successfully* detected unfairness. We follow this convention from existing literature, e.g. (Jung *et al.* 2010, Jung and Cho 2015), to separate the analysis of sensitivity and PPV from that of power. To help build intuition for these metrics, we refer the reader to the toy example provided in Appendix F.

5.4. Configuration of our assessment approach

We apply the *trajectory segmentation* step (Section 4.1) on the compressed trajectories to partition them into stop and move segments. Since the simulator generates routine urban mobility, we argue that this step should identify meaningful stays at recurrent locations such as home, work, shopping, or dining places, rather than short pauses during movement. Accordingly, and in the spirit of stay-point formulation from Hariharan and Toyama (2004), we set the maximum distance from the stay anchor point to 50 meters and the minimum stay duration to 10 minutes. Table 2 summarizes the characteristics of the synthetic movement data and the stop segments.

Table 2. Movement data and stop segments characteristics.

Objects (trajectories)	100,000
Sampling rate	2 minutes
Temporal interval	10 days
Number of trajectory samples	720,199,539
Area of the trajectories’ bounding box	$(4.69 \times 4.83)km^2$
Daily median number of stops per object	4.6 ± 1.43
Stop median duration	122 ± 472.49 minutes

Concerning the geographic zonings (Section 4.2), we use uniform grids with square cells. The set of resolutions was chosen to cover the range of geographic scales that are meaningful in the study area, following the guidelines in Section 4.2. At the lower end, 50 meters approximates the scale of the smallest relevant geographic units, which we consider to be the city blocks. At the upper end, 1000 meters reflects the guideline that a zoning should not be so coarse that a single cell can contain more than half of the population – in our setting, this corresponds to more than half of the population having at least a stop segment falling within the same cell. The intermediate resolutions were

chosen to progressively cover the range between these two extremes, with finer spacing at smaller scales and coarser spacing at larger ones. This choice reflects the fact that changes in resolution matter more at fine geographic scales, while at coarser scales the goal is to capture broader spatial aggregations. Finally, for each resolution X , we shift the grid boundaries rightward and upward by an offset proportional to the resolution, i.e., $\delta \in [0, X)$ with step $X/5$, obtaining 5 grids per resolution. In total, we use 40 different grids.

The *Object-to-cells mapping* step (Section 4.3) maps each object to its top- i , with $i = 8$, cells for each considered grid. We believe that this value is reasonable for the expected number of meaningful places in people’s routines, with some margin for variability. Finally, we instantiate the *hypothesis testing* step (Section 4.5) for the case of assessing binary classifiers, i.e., the step uses the Bernoulli-based spatial scan statistic from Kulldorff (1997). Appendix G provides the details of such instantiation. In line with previous spatial scan statistics literature, e.g., (Read *et al.* 2011, Kulldorff *et al.* 2009, Jung *et al.* 2010), we set the statistical significance level to $\alpha = 0.01$ and the number of Monte Carlo simulations to $n = 999$.

6. Experimental evaluation

In this Section, we evaluate the statistical power, sensitivity, and PPV that our approach achieves across several configurations of datasets. We analyze the results from two complementary perspectives.

The first is a *parameter-wise* perspective, which focuses on how the parameters of the unfairness injection protocol affect the performance of our approach. In this perspective, we compare configurations that differ in one protocol parameter while keeping the grid resolution fixed. In the plots, this corresponds to comparing the considered metrics at a given grid resolution, and allows us to study how power, sensitivity, and PPV change when varying a specific parameter. Connected to this perspective, in each batch of experiments, we also report the results obtained by pooling the extreme candidates detected across all grids. This serves the purpose of capturing the advantages and disadvantages of combining evidence across all considered grid resolutions.

The second is a *resolution-wise* perspective, which focuses on the contribution of each grid resolution to the same three metrics. In this perspective, we follow the behavior of each configuration across grid resolutions. In the plots, this corresponds to reading each curve from finer to coarser grid resolutions. This allows us to study which resolutions favor unfairness detection, which ones favor the retrieval of objects treated unfairly, which ones favor the spatial localization of unfairness, and the various trade-offs one encounters.

6.1. Number of objects per hotspot

We consider five configurations of 1,000 unfair auditable datasets each, where we vary the number of objects associated with a hotspot across the configurations. All the other parameters are kept at their default values (Table 1). As this parameter grows, we expect the unfairness signal to become easier to detect, but precise localization to become harder because hotspots also grow spatially and develop longer boundaries. Results are shown in Figure 3 and Table 3.

Let us consider statistical power. Parameter-wise, it increases with the number of objects per hotspot, as expected. Furthermore, Table 3 shows that pooling the candi-

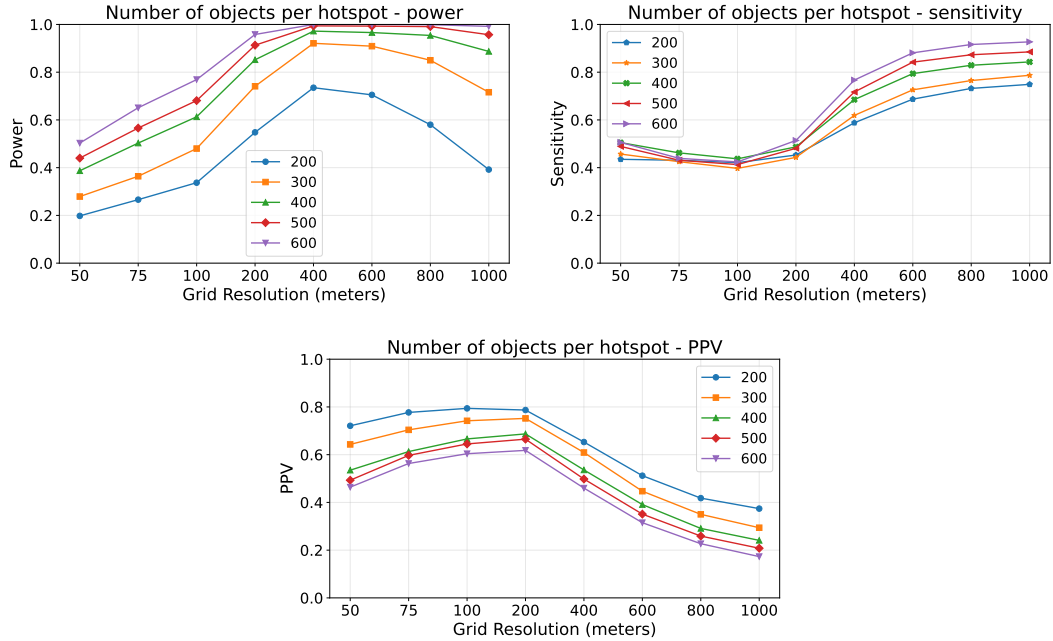


Figure 3. Varying the number of objects per hotspot.

dates deemed extreme from all grids exhibits the same trend and maximizes power, thus proving to be a beneficial strategy for unfairness detection. Resolution-wise, the best-performing resolution depends on the number of objects. This suggests that increasing this parameter also tends, on average, to increase hotspot extent, thereby shifting the most suitable resolution. This is an MAUP effect: the best resolution is scenario-dependent, and even within one scenario, different hotspots may be better captured at different resolutions. Finally, observe that the best performing resolutions fall between 400 and 800 meters, which we argue is due to the average extent of the generated hotspots.

Table 3. Varying the number of objects per hotspot. Power, sensitivity, and PPV when pooling all the extreme candidates from all grids.

Objects per hotspot	Power	Sensitivity	PPV
200	0.904	0.773	0.384
300	0.986	0.866	0.262
400	0.998	0.926	0.193
500	1.000	0.956	0.162
600	1.000	0.975	0.135

Let us now consider sensitivity. Parameter-wise, we see that it remains relatively stable or slightly increases as the number of objects grows. Pooling the extreme candidates from all grids exhibits the same trend. Furthermore, it maximizes this metric, thus proving to be beneficial for the retrieval of the objects treated unfairly. Resolution-wise, sensitivity tends to improve with coarser resolutions: larger cells are more likely to retrieve a larger fraction of unfairly treated objects.

PPV exhibits opposite trends. Parameter-wise, it decreases as the number of objects per hotspot increases. Moreover, pooling the extreme candidates from all grids proves to be even more detrimental, as it ends up considering even more objects that are not

treated unfairly as such. A plausible explanation is that, although larger hotspots are easier to detect, their longer boundaries make it more likely that candidates deemed as extreme include nearby objects that are not actually associated with the hotspots, thus reducing spatial localization precision. Resolution-wise, PPV tends to worsen with coarser resolutions, which can be explained by observing that larger cells are more likely to include objects that do not belong to the hotspots.

Overall, the best trade-off among power, sensitivity, and PPV depends on the number of objects per hotspot and grid resolution. This should not be read as evidence that some resolutions are better, but that different resolutions better match hotspots with different characteristics. Moreover, when candidates are progressively added from the finest to the coarsest resolutions, power and sensitivity increase, but PPV does not. In other words, unfairness detection and the retrieval of objects treated unfairly benefit from this strategy, but at the cost of a negative impact on the spatial localization of unfairness.

6.2. Unfairness magnitude

We consider the five configurations of 1,000 unfair auditable datasets each, in which we vary the magnitude of the unfairness injected into the hotspots. We expect stronger unfairness to be easier to detect, but also to make boundary localization harder, because candidate subsets of cells intersecting hotspot boundaries may increasingly be judged unfair. Results are shown in Figure 4 and Table 4.

Let us consider statistical power. Parameter-wise, it increases with magnitude at every grid resolution, which is expected. The same happens when pooling the extreme candidates from all grids, which also maximizes power thus proving again to be a beneficial strategy for this metric. Resolution-wise, the best performing resolutions concentrate between 400 and 800 meters, which we again argue is due to the average extent of the

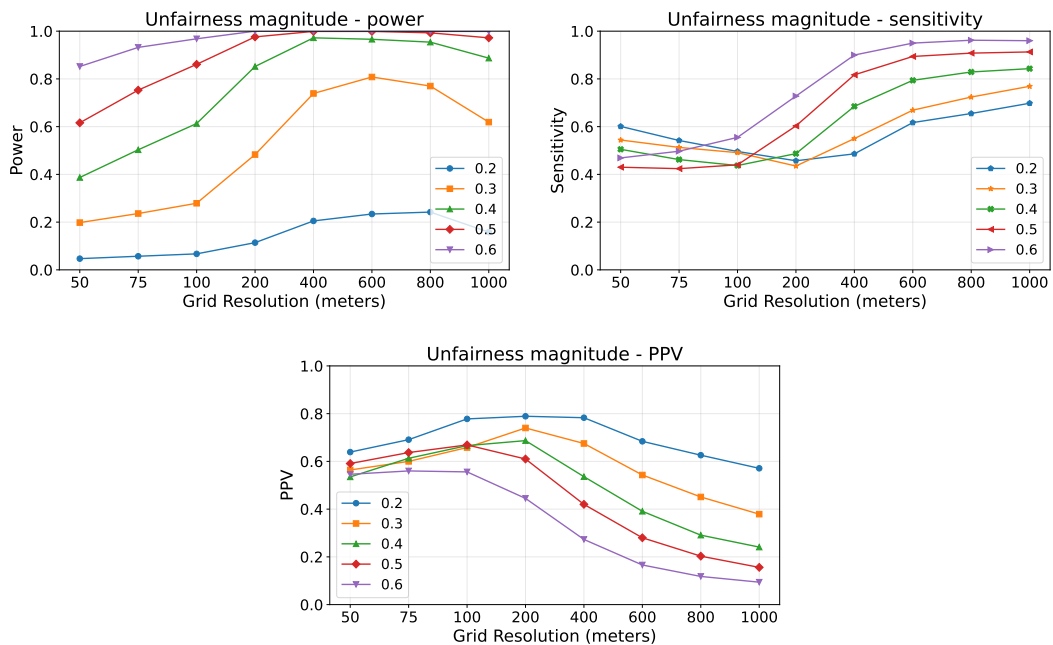


Figure 4. Varying the unfairness magnitude.

generated hotspots.

For what concerns sensitivity, parameter-wise it tends to increase as the magnitude increases across most grid resolutions. The same happens when pooling the extreme candidates from all grids, which also maximizes sensitivity thus proving again to be a beneficial strategy for this metric. We argue that as hotspots become more evident, their objects are more likely to be recovered. Resolution-wise, the best performing ones fall above 400 meters, which we argue is due to the average extent of the generated hotspots.

Table 4. Varying the unfairness magnitude. Power, sensitivity, and PPV when pooling all the extreme candidates from all grids.

Unfairness magnitude	Power	Sensitivity	PPV
0.2	0.451	0.671	0.595
0.3	0.942	0.816	0.352
0.4	0.998	0.926	0.193
0.5	1.000	0.975	0.117
0.6	1.000	0.993	0.065

Finally, consider PPV. Parameter-wise, it tends to decrease as unfairness magnitude increases. This decrease is even more evident when extreme candidates from all resolutions are pooled, which again proves that this strategy is detrimental for this metric. Overall, the results confirm that stronger unfairness not only makes hotspots easier to detect, but also strengthens the signal in candidates intersecting hotspot boundaries; these candidates are therefore more likely to include objects that do not belong to the hotspots, hence lowering PPV, and becomes an especially evident phenomenon with coarser resolutions. Resolution-wise, the best-performing resolutions are the finer ones, i.e., those between 50 and 200 meters. We argue that finer resolutions are likely to include fewer objects that are not treated unfairly, which permits better recognition of the boundaries of the hotspots as unfairness magnitude grows. Overall, we observe again that coarse resolutions mainly help power and sensitivity, while finer resolutions help PPV.

6.3. *Number of hotspots per dataset*

We now consider the three configurations of 1,000 unfair auditable datasets each, in which we vary the number of hotspots per dataset. We expect detection to become easier but localization to become harder, since the approach must deal with hotspots with increasingly more complex boundaries. Results are shown in Figure 5 and Table 5.

Table 5. Varying the number of hotspots per dataset. Power, sensitivity, and PPV when pooling all the extreme candidates from all grids.

Hotspots per dataset	Power	Sensitivity	PPV
1	0.998	0.926	0.193
2	1.000	0.934	0.163
3	1.000	0.934	0.155

Let us first consider statistical power. Parameter-wise, power increases with the number of hotspots, as expected. The same trend is observed when pooling the extreme candidates from all grids; in this case, power is also maximized. Resolution-wise, the

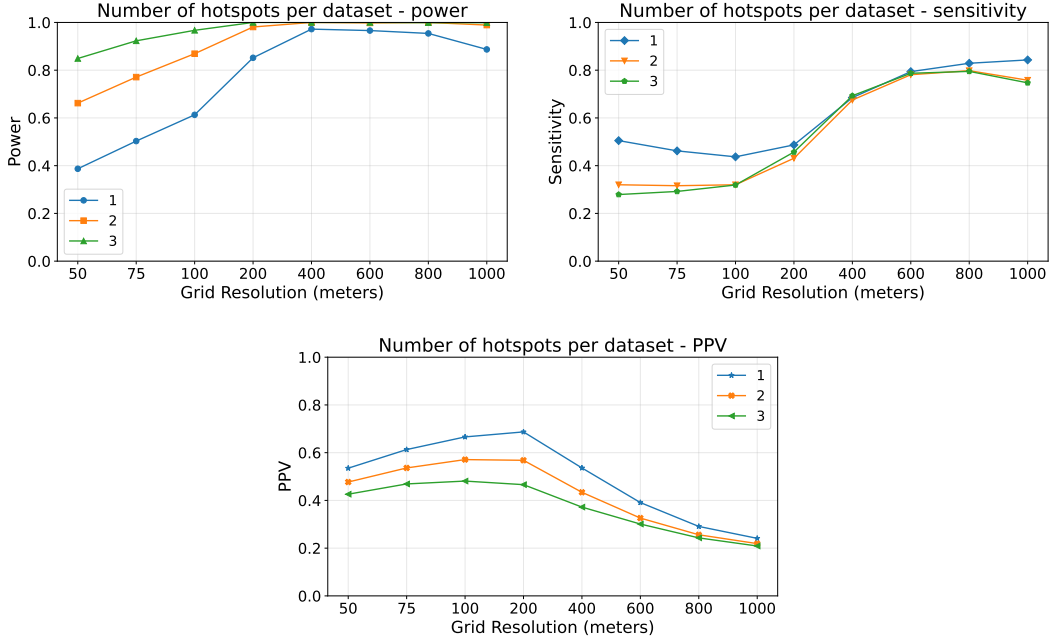


Figure 5. Varying the number of hotspots per dataset.

best-performing resolutions fall between 400 and 800 meters. Furthermore, observe that as we move from finer to coarser resolutions, the gap between the three configurations tends to narrow. We conjecture that finer grid resolutions tend to fragment hotspots more across grid cells. Consequently, adding more hotspots increases the chance that at least one of them, or part of one, aligns well with a grid and yields a statistically significant candidate. With coarser resolutions, instead, even the single-hotspot configuration is often aggregated enough to produce a sufficiently strong unfairness signal. Overall, the results suggest that resolutions that are coarse enough to aggregate the unfairness signal, while not being so coarse as to dilute it, favor unfairness detection.

Sensitivity exhibits different trends. Parameter-wise, for finer grid resolutions below 200 meters, sensitivity tends to decrease moderately as the number of hotspots increases. For coarser resolutions, instead, it remains fairly stable, with only moderate fluctuations. This suggests that as the number of hotspots increases, the retrieval of objects that are treated differently might become more difficult, at least when using certain grid resolutions. When the extreme candidates from all grids are pooled, sensitivity is maximized again. Resolution-wise, the best-performing resolutions are the coarser ones, which suggests again that they represent the better choice when targeting the retrieval of objects that are treated differently.

Finally, consider PPV. Parameter-wise, it decreases as the number of hotspots increases, which is expected. The same is observed when the extreme candidates from all grids are pooled, which again proves to be detrimental to this metric. Resolution-wise, the best-performing resolutions are the finer ones, with the 100 and 200 meter resolutions achieving the highest PPV. The results again suggest that finer resolutions represent the better choice when targeting precise spatial localization of unfairness.

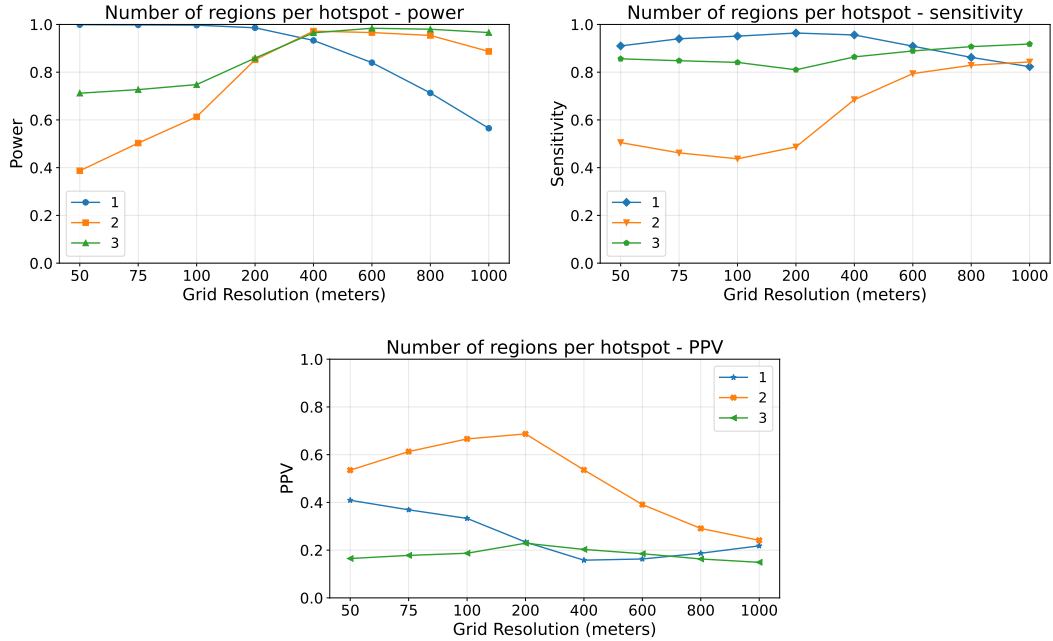


Figure 6. Varying the number of regions per hotspot.

6.4. Number of regions per hotspot

We consider the three configurations of 1,000 unfair auditable datasets each, in which we vary the number of regions composing each hotspot. Increasing the number of regions does not increase the number of associated objects, but it requires those same objects to be associated with more distinct regions; as a result, hotspot regions tend to become larger and their boundaries more complex. Results are shown in Figure 6 and Table 6.

Table 6. Varying the number of regions per hotspot. Power, sensitivity, and PPV when pooling all the extreme candidates from all grids.

Regions per hotspot	Power	Sensitivity	PPV
1	1.000	0.990	0.105
2	0.998	0.926	0.193
3	0.996	0.961	0.102

Let us first consider statistical power. Parameter-wise, the effect of increasing the number of regions depends on the grid resolution. At finer resolutions, i.e., below 400 meters, power decreases as the number of regions increases. At coarser resolutions, the opposite trend emerges. Resolution-wise, the one-region case behaves differently from the two- and three-region cases: power decreases as the grid becomes coarser for one-region hotspots, whereas it increases for hotspots composed of two or three regions. We interpret the results from both perspectives as a scale-matching effect. One-region hotspots are more compact, and are therefore better captured by finer grids. When the grid becomes too coarse, the unfairness signal is diluted by objects that are not truly associated with the hotspot, which reduces power. By contrast, hotspots composed of two or three regions have a larger spatial extent, and in these cases coarser grids are better able to aggregate enough of the objects treated differently to reveal the unfairness signal. Overall, the best-performing resolution tends to become coarser as the number

of regions increases. As in the previous experiments, pooling the extreme candidates from all grid resolutions maximizes power.

For sensitivity, parameter-wise the results suggest an interesting non-monotonic effect of the number of regions per hotspot, in part already observed while focusing on statistical power: objects associated with one- or three-region hotspots appear to be generally easier to retrieve than the two-region case. The same is observed when pooling the extreme candidates from all grid resolutions, which again maximizes sensitivity. On the one hand, observe that the unfairness signal of one-region hotspots is *spatially compact*, hence we argue that all grid resolutions, and especially the finer ones, tend to generate candidates that can retrieve most of the objects treated unfairly. On the other hand, the three-region hotspots are spatially more fragmented, which can negatively impact object retrieval, in particular with finer grid resolutions. At the same time, they also provide more regions from which the same objects that are treated unfairly can be retrieved by the candidates deemed extreme, thus favoring object retrieval across all grid resolutions. The two-region case appears to sit in an intermediate situation: it is sufficiently fragmented such that finer grids may split the affected objects across several candidate subsets, but not fragmented enough to provide the same number of retrieval opportunities as the three-region case, leading to the worst results observed for this metric. Resolution-wise, sensitivity tends to increase with grid resolution for the two-region case, while for the other cases it remains fairly stable, which we argue is due to the reasons explained above. Overall, the results suggest once more that coarser resolutions represent the better choice when retrieving the set of objects that are treated differently.

Let us finally consider PPV. Parameter-wise, the results highlight again a non-monotonic effect of the number of regions per hotspot. We argue that two contrasting phenomena are involved. On the one hand, increasing the number of regions can improve PPV because the unfair movement pattern becomes more selective: fewer unaffected objects are likely to be associated with the same set of regions making up a hotspot. On the other hand, as the number of regions increases, hotspots become more spatially fragmented, hence their boundaries become more complex. As a result, candidates deemed extreme may include objects that are not associated with the hotspots, therefore reducing PPV. Finally, pooling the extreme candidates from all grids proves to be detrimental once more. Resolution-wise, the best performing resolutions are the finer ones, in line with the previous results.

6.5. *Number of object stops per hotspot region*

We consider the three configurations of 1,000 unfair auditable datasets each, in which we vary the number of stop centroids required for an object to be associated with each hotspot region. Increasing this parameter should, on average, enlarge hotspot regions and complicate their boundaries, potentially making both detection and localization harder. On the other hand, it might also facilitate the object-to-cells mapping step of our approach, thus improving performance. Results are shown in Figure 7 and Table 7.

Let us consider statistical power. Parameter-wise, we observe minimal fluctuations, which suggests that the object-to-cells mapping step from Section 4.3 is resilient to variations in this parameter. At the same time, this may also depend on properties of the movement data being considered, such as the spatial distribution of the stop centroids. Finally, pooling the extreme candidates from all grid resolutions maximizes power. Resolution-wise, coarser resolutions perform the best, in line with the trends

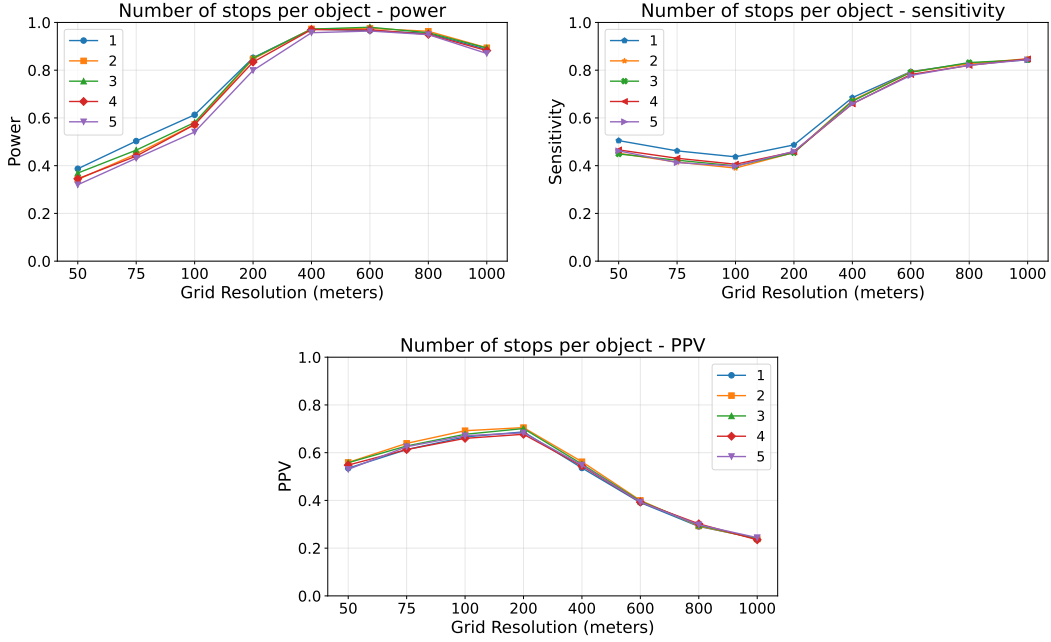


Figure 7. Varying the number of stops per hotspot region.

observed in the previous experiments.

Sensitivity follows similar trends, parameter-wise and resolution-wise. Finally, PPV behaves similarly parameter-wise, while resolution-wise the best performing resolutions are the finer ones, which is in line with the results observed in the previous experiments.

Table 7. Varying the number of stops per hotspot region. Power, sensitivity, and PPV when pooling all the extreme candidates from all grids.

Object stops per hotspot region	Power	Sensitivity	PPV
1	0.998	0.926	0.193
2	0.996	0.929	0.193
3	0.999	0.927	0.196
4	0.999	0.919	0.200
5	0.996	0.919	0.200

6.6. Discussion

An important practical question at this point is: *what should one do in a real-world assessment?* That is, when one does not know whether there are hotspots, which shapes or spatial scales they have or how best to balance power, sensitivity, and PPV.

In order to address this question, we outline a practical exploratory strategy based on the patterns that emerged repeatedly throughout the experimental evaluation. First, we argue that such a strategy should begin by pooling the candidates deemed extreme from all grids. This prioritizes unfairness detection: if no extreme candidate is found at any resolution, then there is no evidence of unfairness based on movement patterns. Conversely, if at least one extreme candidate is found, this provides statistical evidence that unfairness is present, and the analysis must proceed to inspect the objects belonging to the extreme candidates and investigate where the unfairness may be spatially

localized.

Next, recall from the experimental evaluation’s findings that coarser resolutions mainly support power and sensitivity, while finer ones mainly support precise unfairness spatial localization and thus PPV. Consequently, we suggest beginning with coarse resolutions, which provide a broad indication of where unfair hotspots may be located and facilitate the retrieval of objects treated unfairly. Subsequently, one should turn to finer resolutions to refine those areas and restrict the set of objects deemed as treated unfairly, but only when such resolutions offer a clear and spatially consistent refinement of the same hotspots. Finally, if hotspots exist at different spatial scales, separate resolution ranges may need to be examined.

7. Searching for potential unfairness: a sample case

We now illustrate how the exploratory strategy outlined in the previous discussion can be used in a real-world assessment. We randomly select one auditable dataset from the experiments but we do not inspect its characteristics, as we aim to verify whether the strategy can correctly guide the assessment, and thus reveal the true hotspots.

We begin by executing our assessment approach on the dataset, configuring it according to the parameters described in Section 5.4. We first verify whether its final output, $UNFAIR_{GZ} \neq \emptyset$, i.e., contains at least one candidate subset deemed extreme. Observe that this follows the strategy of pooling extreme candidates across all resolutions, which maximizes unfairness detection (i.e., statistical power). Being that the case, we now know that there is statistical evidence that unfairness is present and further investigation is required.

Next, we consider the extreme candidate subsets detected at coarse resolutions, with the aim of favoring object retrieval (i.e., sensitivity). Using only the 1000-meter grids,

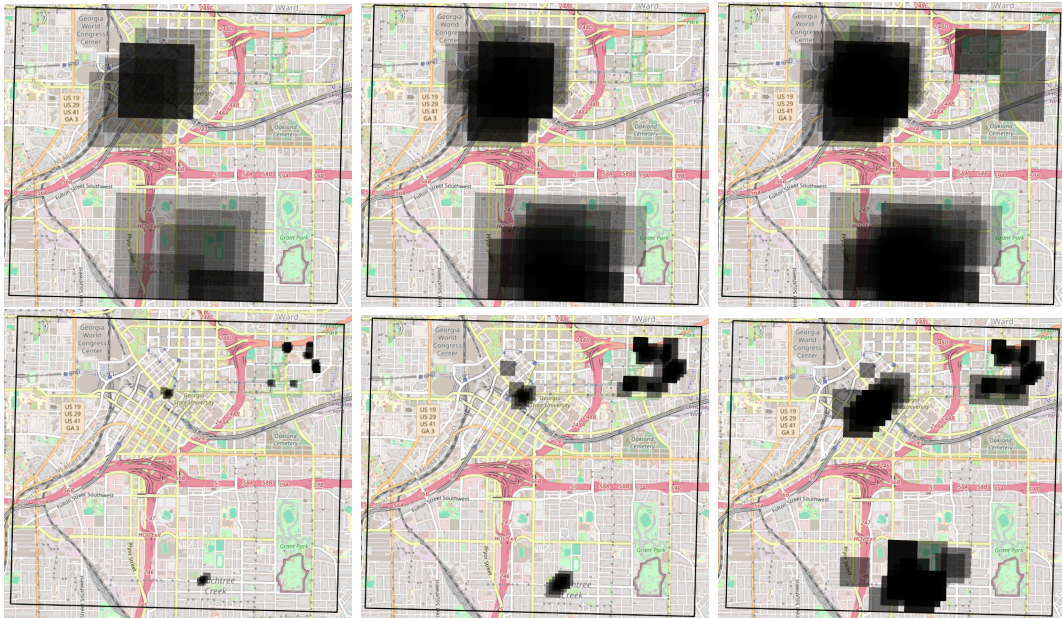


Figure 8. The plots in the *top row* show the cells, i.e., the gray-shaded areas, belonging to the extreme candidates detected at coarser grid resolutions. The plots in the *bottom row* show the cells belonging to candidates detected at finer grid resolutions. The darker an area is, the more it is covered by cells from extreme candidates. The black rectangle represents the bounding box containing the movement data.

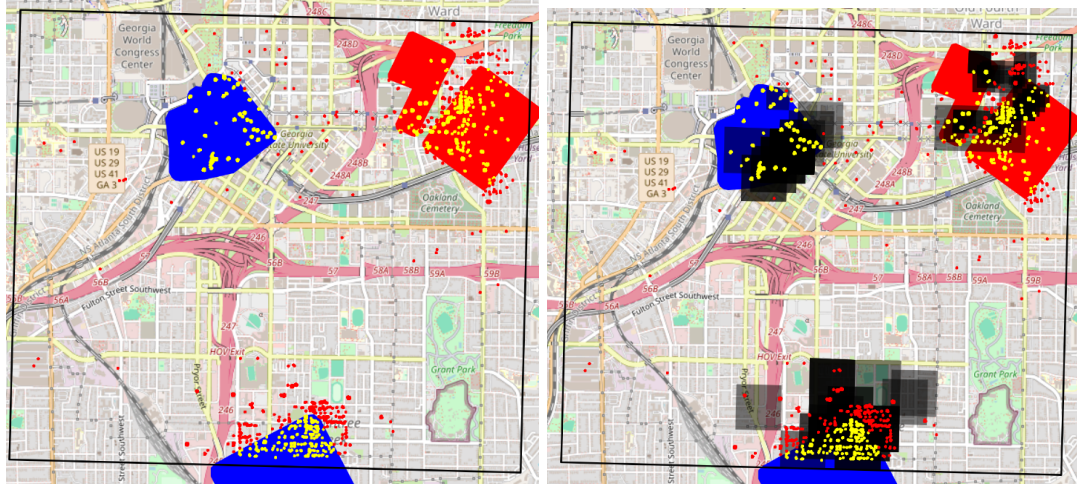


Figure 9. The *left plot* shows the two actual hotspots, each composed of two regions, highlighted in blue and red, respectively. The yellow and red points show the stop centroids of the objects associated with the hotspots: yellow points fall within the hotspot regions, while red points fall outside them. The *right plot* superimposes, on the hotspots, the cells belonging to the extreme candidates detected from the 50-, 75-, 100-, 200-, and 400-meter grid resolutions, shown as gray-shaded areas, together with the stop centroids.

two broad areas emerge (Figure 8, top-left). Adding the 800-meter grids makes these areas slightly larger (Figure 8, top-middle), strengthening the conclusion that unfairness is roughly localized there. When the 600-meter grids are also added (Figure 8, top-right), a third broad area appears. This suggests that unfairness may thus be located in these three areas. We now turn to the finer resolutions, with the aim of favoring unfairness spatial localization (i.e., PPV). Using finer grids, e.g., 50-, 75-, and 100-meter resolution, highlights areas within the larger areas previously identified (Figure 8, bottom-left). Adding the 200-meter grids makes the smaller areas begin to coalesce into larger ones (Figure 8, bottom-middle). Finally, adding the 400-meter grids makes all three areas coalesce further and enlarge (Figure 8, bottom-right).

At this point we look at the true hotspots in the auditable dataset, with the intent to verify if our strategy has indeed found out areas in which there is unfairness. Recall from Section 5.2 that, in our generation protocol, each hotspot is generated independently and may be composed of multiple distinct regions. Recall also that an object is associated with that hotspot only if it has at least a given number of stop centroids in each of those regions. Hence, in the plots below, each color denotes one specific hotspot while the disconnected polygons with the same color denote the regions composing it. Figure 9, left plot, shows that there are two hotspots, each composed of two distinct regions, highlighted in blue and red respectively. The figure also shows the stop centroids of the objects associated with the hotspots: the yellow centroids fall within the hotspot regions, while the red ones fall outside. Figure 9, right plot, then superimposes the gray areas, i.e., the cells belonging to the extreme candidates detected from the 50- to the 400-meter grids, over the two hotspots. This plot shows that the three detected areas, in fact, roughly cover the regions of the hotspots.

We finally consider the stop centroids falling outside the hotspot regions, represented by the red dots in Figure 9. Observe that the detected candidates cover areas outside the true hotspots, which might initially be interpreted as poor spatial localization of unfairness. However, note that part of these areas actually contain many of those outside (red) centroids. In turn, those centroids highlight that unfairly treated objects in reality have broader movement patterns than those defined by the hotspot-triggering

regions alone. We thus argue that our assessment approach has correctly determined the presence of unfairness in those specific areas.

Overall, we argue that our practical exploratory strategy provides a reasonable approximation of the areas that warrant deeper investigation.

8. Conclusions

In this work, we introduced the problem of assessing predictive models for fairness based on movement patterns. We also proposed an approach to address this problem and evaluated it experimentally in the case of assessing binary classifiers. To this end, we first introduced a protocol to generate synthetic auditable datasets, and then evaluated its detection, object retrieval, and localization performance with respect to several parameters. The results suggest that our approach is effective at detecting unfairness based on movement patterns and at retrieving the objects treated unfairly, while also providing useful localization performance. The results also highlight multi-resolution trade-offs between unfairness detection, object retrieval, and precise localization of unfairness. Accordingly, we suggest an exploratory strategy when dealing with real-world assessments. Finally, we note that our proposed approach can be specialized to address the spatial fairness assessment scenario where individuals are tied to a single location, thus being generic in nature.

There are multiple directions of future research. First, it would be useful to move beyond the uniform square grids adopted in our study and previous related works, and investigate alternative tessellations, e.g., data-driven or density-aware ones such as those obtained with DBSCAN (Schubert *et al.* 2017): these may better reflect the spatial distribution of movement data, thus improving all the considered metrics. Closely related is the shape of the cells in the tessellations: the spatial scan statistics literature has long shown that detection performance is sensitive to their geometries (Tango and Takahashi 2005).

A second direction is to improve the reporting of the candidate subsets of cells deemed extreme, with the goal of improving unfairness spatial localization and benefiting the exploratory strategy. Similar problems have been studied in the spatial scan statistics literature (e.g., using the Gini coefficient, such as in Han *et al.* (2016)), hence it would be interesting to apply these ideas within our setting.

A third direction concerns how objects are associated with cells. In our work, this is based on stop segments, but alternative criteria, such as those that consider move segments, might be more effective in different scenarios. Another direction could develop richer and more varied unfairness injection protocols, investigate movement data with different characteristics, and consider assessing other types of predictive models (e.g., regression, multi-class classification).

References

- Agrawal, R., *et al.*, 1996. Fast discovery of association rules. *Advances in knowledge discovery and data mining*, 12 (1), 307–328.
- Caton, S. and Haas, C., 2024. Fairness in machine learning: A survey. *ACM Comput. Surv.*, 56 (7).
- Dwork, C. and Ilvento, C., 2018a. Group fairness under composition. *In: Proceedings of the Conference on Fairness, Accountability, and Transparency*. vol. 3.

- Dwork, C. and Ilvento, C., 2018b. Individual fairness under composition. *Proceedings of fairness, accountability, transparency in machine learning, 2018*.
- Ensign, D., et al., 2018. Runaway feedback loops in predictive policing. In: *Proceedings of the 1st Conference on Fairness, Accountability and Transparency*. vol. 81, 160–171.
- Friedler, S.A., et al., 2019. A comparative study of fairness-enhancing interventions in machine learning. In: *Proceedings of the conference on fairness, accountability, and transparency*. 329–338.
- Han, J., Pei, J., and Yin, Y., 2000. Mining frequent patterns without candidate generation. *ACM sigmod record*, 29 (2), 1–12.
- Han, J., et al., 2016. Using gini coefficient to determining optimal cluster reporting sizes for spatial scan statistics. *International journal of health geographics*, 15 (1), 27.
- Hariharan, R. and Toyama, K., 2004. Project lachesis: parsing and modeling location histories. In: *International Conference on Geographic Information Science*. Springer, 106–124.
- Jung, I. and Cho, H.J., 2015. A nonparametric spatial scan statistic for continuous data. *International journal of health geographics*, 14 (1), 30.
- Jung, I., Kulldorff, M., and Richard, O.J., 2010. A spatial scan statistic for multinomial data. *Statistics in medicine*, 29 (18), 1910–1918.
- Kulldorff, M., 1997. A spatial scan statistic. *Communications in Statistics-Theory and methods*, 26 (6), 1481–1496.
- Kulldorff, M., 2001. Prospective time periodic geographical disease surveillance using a scan statistic. *Journal of the Royal Statistical Society: Series A (Statistics in Society)*, 164 (1), 61–72.
- Kulldorff, M., Huang, L., and Konty, K., 2009. A scan statistic for continuous data based on the normal probability model. *International journal of health geographics*, 8 (1), 58.
- Pappalardo, L., et al., 2022. Scikit-mobility: A python library for the analysis, generation, and risk assessment of mobility data. *Journal of Statistical Software*, 103, 1–38.
- Read, S., et al., 2011. Measuring the spatial accuracy of the spatial scan statistic. *Spatial and spatio-temporal epidemiology*, 2 (2), 69–78.
- Sacharidis, D., et al., 2023. Auditing for spatial fairness. In: *Proceedings 26th EDBT*. 485–491.
- Saxena, N.A., Mathur, R., and Shahabi, C., 2025. Legally-compliant spatial fairness framework: Advancing beyond spatial fairness. In: *Proceedings 28th EDBT*. 842–854.
- Schubert, E., et al., 2017. DBSCAN revisited, revisited: why and how you should (still) use DBSCAN. *ACM transactions on database systems*, 42 (3), 1–21.
- Shaham, S., Ghinita, G., and Shahabi, C., 2022. Models and mechanisms for spatial data fairness. *Proc. VLDB Endow.*, 16 (2), 167–179.
- Spaccapietra, S., et al., 2008. A conceptual view on trajectories. *Data & Knowledge Engineering*, 65 (1), 126–146.
- Tango, T. and Takahashi, K., 2005. A flexibly shaped spatial scan statistic for detecting clusters. *International journal of health geographics*, 4 (1), 11.
- U.S. Census Bureau, Department of Commerce, 2025. TIGER/Line Shapefile, State of Georgia, 2025 Census Block Groups. https://www2.census.gov/geo/tiger/TIGER2025/BG/tl_2025_13_bg.zip. Data.gov catalog entry; accessed 2026-04-26.
- Wong, D.W., 2004. The modifiable areal unit problem (MAUP). In: *Worldminds: geographical perspectives on 100 problems 1904–2004*. Springer, 571–575.
- Xie, Y., et al., 2022. Fairness by “where”: A statistically-robust and model-agnostic bi-level learning framework. *Proceedings of the AAAI Conference on Artificial Intelligence*, 36 (11), 12208–12216.
- Yan, A. and Howe, B., 2021. Equitensors: Learning fair integrations of heterogeneous urban data. In: *ACM SIGMOD*. 2338–2347.
- Zaki, M.J., 2002. Scalable algorithms for association mining. *IEEE TKDE*, 12 (3), 372–390.
- Zheng, Y., 2015. Trajectory data mining: An overview. *ACM Trans. Intell. Syst. Technol.*, 6 (3).
- Züfle, A., et al., 2023. Urban life: a model of people and places. *Computational and Mathematical Organization Theory*, 29 (1), 20–51.

Appendix A. Group fairness targeting statistical parity

Let $\mathcal{A} \in \{0, 1\}$ represent a binary protected attribute defining a group (e.g., sex, race, income level) and where the values 1 and 0 encode membership or not, respectively, to such a group. Let also \hat{Y} be the output of a predictive model for some moving object. Group fairness targeting statistical parity requires

$$d(P(\hat{Y} | \mathcal{A} = 1), P(\hat{Y} | \mathcal{A} = 0)) \leq \epsilon$$

to hold, where $P(\cdot | \cdot)$ is a conditional probability distribution, $d(\cdot, \cdot)$ is a suitable distance measure between probability distributions (e.g., total variation distance), and ϵ is a nonnegative threshold that encodes the maximum disparity deemed acceptable, and in practice is an application- and policy-dependent threshold (Dwork and Ilvento 2018a).

For example, consider a predictive model that is a binary classifier (hence $\hat{Y} \in \{0, 1\}$). Then, the above condition reduces to checking if the probability of an unfavorable output (e.g. $\hat{Y} = 1$) for an individual belonging to the protected group (i.e., $\mathcal{A} = 1$), in other words $P(\hat{Y} = 1 | \mathcal{A} = 1)$, is sufficiently close (i.e., within ϵ) to that of an individual of the non-protected group, $P(\hat{Y} = 1 | \mathcal{A} = 0)$.

Finally, we recall from the literature that targeting exact statistical parity, i.e., $\epsilon = 0$, is not desirable, as it would sacrifice a model’s utility (e.g., accuracy) for total fairness beyond what is reasonable (Dwork and Ilvento 2018a, Friedler *et al.* 2019, Shaham *et al.* 2022).

Appendix B. The Modifiable Areal Unit Problem: an illustrative example

To better illustrate the Modifiable Areal Unit Problem (MAUP), consider the simple example in Figure B1, which shows the case of assessing the spatial fairness of a binary classifier. The top-left plot shows the spatial distribution of the classifier’s outcomes (positive in green, negative in red). We consider 52 individuals: 28 receive a negative outcome and 24 a positive one, yielding a global positive rate of ~ 0.46 and a global negative rate of ~ 0.54 . Our goal is to determine whether these global rates also hold locally, or whether there exist areas in which the classifier behaves differently: we call these areas *hotspots of unfairness*. In practice, this requires identifying regions where the local positive/negative rates differ significantly from the global ones.

In the top-left plot of Figure B1, the area highlighted in red provides an example of a hotspot: it contains individuals receiving predominantly negative outcomes (local rates: negative 0.9, positive 0.1). Unfortunately, the shape and location of hotspots of unfairness are not known *a priori*. As a result, relying on a single spatial partition would fail to detect localized instances of unfairness.

Figure B1’s top-right plot shows exactly this failure. Using a 1×2 uniform grid, the cell containing the hotspot also includes many surrounding points: this makes the cell’s local negative (~ 0.57) and positive (~ 0.43) rates remain close to the global ones, and the unfairness is not detected. Therefore, to mitigate the MAUP, related works typically repeat the assessment over multiple partitions with different resolutions and alignments, and then combine the evidence across partitions.

For instance, consider the 1×4 grid used in the bottom-left plot. Here, one cell isolates the hotspot more effectively, producing a clear discrepancy between the local and global rates. However, varying resolution alone may still be insufficient; changing

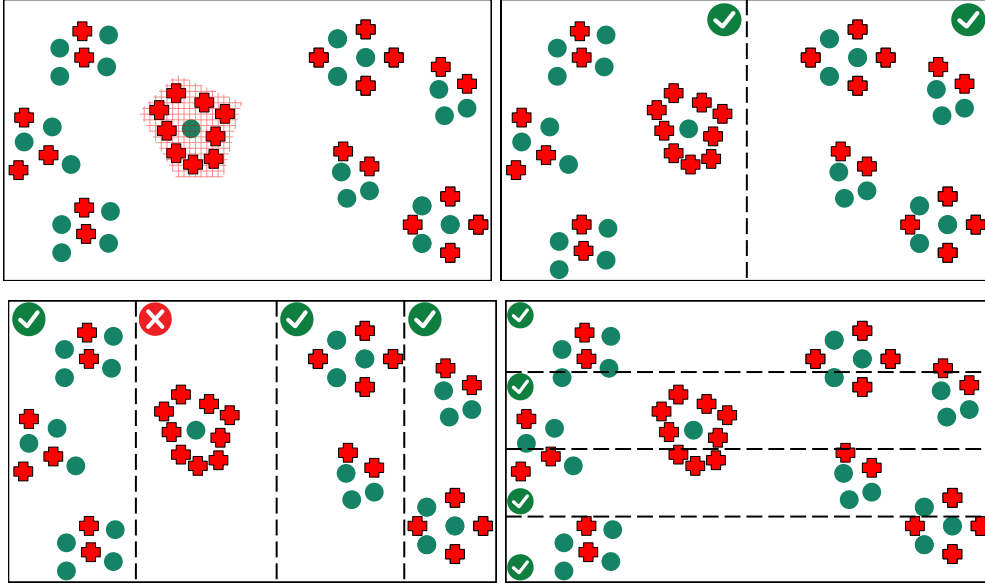


Figure B1. Simple example illustrating the Modifiable Areal Unit Problem when assessing the spatial fairness of a binary classifier with respect to possible different partitionings. A positive (negative) outcome is denoted in green (red).

the grid alignment can be crucial as well. This is illustrated by the 4×1 grid used in Figure B1’s bottom-right plot, where the local rates within each cell remain close to the global ones, and the hotspot is not detected.

Overall, this simple example shows how different partitions with varying resolutions and alignments can be used to deal with the MAUP. It also motivates the need to combine evidence gathered across multiple partitions to draw final conclusions. The same considerations apply to the problem of assessing predictive models for fairness based on movement patterns. Let us therefore go back to defining this problem.

Appendix C. Further details on the step of computing the subsets of cells that must undergo hypothesis testing

The Eclat-like algorithm (Zaki 2002) we implemented to determine the subsets of cells that must undergo hypothesis testing is a (1) *bottom-up* approach, in that it finds frequent subsets of cells of cardinality k by joining the frequent subsets of cardinality $k-1$ found during the previous iteration; (2) the support of a subset of cells is computed as the cardinality of the intersection between the sets of moving object IDs associated with the subsets being joined; (3) it is a *prefix-based* approach, meaning that each cell is assigned a unique ID, enabling lexicographic sorting of subsets of cells, i.e., the prefixes⁴. This, in turn, allows efficient partitioning of the search space by reducing redundant joins. Finally, while more efficient algorithms than Eclat-like ones exist, e.g., those targeting maximal itemsets to speed up the computation of candidate itemsets (Han *et al.* 2000, Zaki 2002)), an Eclat-like algorithm integrates very well with our assessment framework.

Finally, we highlight a theoretical result from (Zaki 2002) that applies to Eclat-like

⁴We report that each prefix technically corresponds to an equivalence class, as introduced in the Definition 8 from (Zaki 2002).

algorithms. Among the corollaries of Theorem 3, the author observes that if V is the number of transactions and the largest transaction has length i , then all itemsets can be enumerated and checked for support in time $O(2^i V)$: hence, for sufficiently small values of i , the overall complexity grows approximately linearly with the number of transactions, $\sim O(V)$. Recall then that, during the *Object-to-cells mapping* step, our approach explicitly controls the maximum size i a moving object’s cellset GZ_{mo}^i can have. This implies that our assessment approach directly *bounds* the largest possible transaction size, and when stop segments are used as the basis for the object-to-cells mapping step (as we do in this work), i can be expected to be reasonably small.

Appendix D. Observations on the complexity of the hypothesis testing step

The overall complexity of the hypothesis testing step is dominated by the n Monte Carlo simulations needed to derive an approximated distribution of T under H_0 , i.e., $O(|PRED| \times |CANDIDATES_{GZ}| \times n)$. More specifically, for each simulation $b \in \{1, \dots, n\}$ we need to compute the test statistic T . This requires to first permute the predicted values, which has cost $O(|PRED|)$; and then compute $L_1^{max}(CANDIDATES_{GZ}, PRED_b)$, which requires, for every subset $c \in CANDIDATES_{GZ}$, to aggregate the predicted values of the moving objects associated with c and the predicted values of the other moving objects. The cost per subset c is $O(|PRED|)$, hence evaluating L_1^{max} for all subsets $c \in CANDIDATES_{GZ}$ has cost $O(|CANDIDATES_{GZ}| \times |PRED|)$. Finally, observe that computing $L_0^{max}(PRED)$ can be done just once, and the result can be shared across the simulations. Therefore, each simulation has cost $O(|CANDIDATES_{GZ}| \times |PRED|)$.

Appendix E. Overall complexity of the proposed approach

Let us briefly discuss the overall complexity of our assessment approach. Let S_1 be the trajectory segmentation step, S_2 the geographic zoning step, S_3 the object-to-cells mapping step, S_4 the step that computes the subsets of cells that must undergo hypothesis testing, and S_5 the hypothesis testing step. If we denote as q the number of geographic zonings used, then the overall complexity of our approach is:

$$O(S_1 + S_2 + q \cdot (S_3 + S_4) + S_5).$$

In practice, we highlight that the time-dominant steps are S_3 , S_4 , and S_5 . However, observe that S_3 and S_4 are embarrassingly parallel with respect to the different zonings, while S_5 is embarrassingly parallel with respect to the Monte Carlo simulations (i.e., the time-dominant component within that step). Consequently, increasing the computational resources allocated to these steps reduces their execution time.

Appendix F. Understanding sensitivity and positive predictive value (PPV): a toy example

To help the reader develop intuition on these two metrics, consider a dataset containing 100,000 moving objects, and suppose that unfairness has been injected through their labels such that there is a hotspot of unfairness composed of two distinct regions. Assume

that this hotspot is associated with 600 objects, i.e., these 600 objects are associated with its two regions and are treated differently because of this. Now suppose that our assessment approach uses a set of uniform grids (geographical zonings) with different resolutions and alignments, and returns from the various grids a collection of subsets of cells that are deemed extreme. Assume further that the total number of objects associated with any of these subsets is 1,000, and that 300 of these objects actually belong to the hotspot. Then, sensitivity is equal to 0.5 and PPV to 0.3.

Consider now a limit case, in which we artificially make the assessment approach return the entire set of 100,000 objects whenever it detects unfairness. In this case, sensitivity would be a perfect 1, but PPV would be only 0.003, indicating that localization performance is, effectively, compromised. Consider finally a second limit case, in which the assessment approach always returns objects belonging to a hotspot, but only a small fraction of them; for instance, suppose that it returns only 30 of the hotspot’s 600 objects. In this case, the approach would achieve a perfect PPV of 1, but its sensitivity would only be 0.05, which indicates another type of poor localization performance.

In general, observe the tension between sensitivity and PPV: they capture complementary aspects of localization. High sensitivity with low PPV indicates that the detected hotspot(s) covers a large portion of the true unfair hotspot(s) but extends substantially into non-unfair areas. In contrast, high PPV with low sensitivity indicates that the detected hotspot(s) is spatially precise, but captures only a limited portion of the true unfair hotspot(s)’s extent.

Appendix G. Hypothesis testing when assessing a binary classifier for fairness based on movement patterns.

We first state the null and alternative hypotheses (Stage 1). Next, we select the scan statistic appropriate for assessing binary classifiers for fairness based on movement patterns, i.e., the Bernoulli-based spatial scan statistic from (Kulldorff 1997) (Stage 2). Under the Bernoulli model, both hypotheses are expressed through the binomial parametric probability model $\binom{N}{k}\theta^k \times (1 - \theta)^{N-k}$, where N is the number of trials, k the number of successes, and θ the probability of success.

We then formalize H_0 as the likelihood function L_0 using the above-mentioned parametric probability model (stage 3):

$$L_0(\theta, PRED) = \theta^{p(PRED)} \times (1 - \theta)^{n(PRED)-p(PRED)}$$

Here, $n(PRED)$ is the number of labels (moving objects) in $PRED$ and $p(PRED)$ is the number of positive labels in $PRED$. Note that the binomial coefficient is omitted from both L_0 and L_1 , since it would cancel out in the likelihood ratio. Then, computing L_0^{max} requires finding the MLE $\hat{\theta}$, which in this case has closed form as it can be obtained by finding the solution for the derivative $dL_0/d\theta = 0$ (observe that in reality one works with the logarithm of L_0 for numerical stability): this yields $\hat{\theta} = p(PRED)/n(PRED)$.

Next (Stage 4), we formalize H_1 as the likelihood function L_1 :

$$\begin{aligned} L_1(\theta_{in}, \theta_{out}, c, PRED) = & \\ & \left(\theta_{in}^{p(c)} \times (1 - \theta_{in})^{n(c)-p(c)} \right) \times \\ & \left(\theta_{out}^{p(PRED)-p(c)} \times (1 - \theta_{out})^{n(PRED)-n(c)-(p(PRED)-p(c))} \right). \end{aligned}$$

Observe that the binomial parametric probability model is used twice in L_1 : the first factor (second row) models the distribution of the labels over the moving objects associated with a subset of cells c , while the second term (third row) models the distribution of the labels over the other moving objects. To compute L_1^{max} we then proceed as follows: first, for every $c \in CANDIDATES_{\mathcal{GZ}}$ we compute $L_1^{max}(c, PRED)$, which requires to compute the MLEs $\hat{\theta}_{in}^c$ and $\hat{\theta}_{out}^c$. These, in turn, are found by finding the solution for the partial derivatives:

$$\frac{\partial(L_1(\theta_{in}^c, \theta_{out}^c, c, PRED))}{\partial\theta_{in}} = 0$$

$$\frac{\partial(L_1(\theta_{in}^c, \theta_{out}^c, c, PRED))}{\partial\theta_{out}} = 0.$$

Note that, as said previously, in practice one works with the logarithm of L_1 . Thus, we get $\hat{\theta}_{in}^c = p(c)/n(c)$ and $\hat{\theta}_{out}^c = (p(PRED) - p(c))/(n(PRED) - n(c))$. Finally, $L_1^{max}(CANDIDATES_{\mathcal{GZ}}, PRED)$ is obtained by selecting $c^* \in CANDIDATES_{\mathcal{GZ}}$ that yields the largest $L_1^{max}(c, PRED)$.

The remaining operations follow the Stages 5-9 of the process verbatim, i.e., we set the desired significance level α (Stage 5), then compute an approximated distribution of the maximum likelihood ratio under H_0 by performing n Monte Carlo simulations (Stage 6), subsequently compute the maximum likelihood ratio over the original predicted values in $PRED$, obtaining T_{obs} (Stage 7), use the approximated distribution and T_{obs} to determine the Monte Carlo p-value \hat{p} needed to decide whether to reject H_0 (Stage 8), and finally store the evidence of movement unfairness (if any) in $UNFAIR_{\mathcal{GZ}}$ (Stage 9).